NASA CR 102686

FORCES DUE TO A COMMAND SERVICE MODULE REACTION CONTROL MOTOR PLUME IMPINGING ON THE SATURN V CLUSTER ARRANGEMENT (Dry Workshop Version)

Lockheed

MISSILES & SPACE COMPANY

A GROUP DIVISION OF LOCKHEED AIRCRAFT CORPORATION

SUNNYVALE, CALIFORNIA

TM 54/20-231
LMSC/HREC D149170

LOCKHEED MISSILES & SPACE COMPANY

HUNTSVILLE RESEARCH & ENGINEERING CENTER

HUNTSVILLE RESEARCH PARK

4800 BRADFORD BLVD., HUNTSVILLE, ALABAMA

FORCES DUE TO A COMMAND SERVICE MODULE REACTION CONTROL MOTOR PLUME IMPINGING ON THE SATURN V CLUSTER ARRANGEMENT (Dry Workshop Version)

August 1969

Contract NAS8-20082

by

M. M. Penny

APPROVED BY: John W Benefield
J. W. Benefield, Supervisor
Propulsion Section

George D. Reny
G. D. Reny, Manager
Aeromechanics Dept.

FOREWORD

This document presents the results of work performed by Lockheed's Huntsville Research & Engineering Center under subcontract to Northrop Nortronics (NSL PO 5-09287) for the Aero-Astrodynamics Laboratory of Marshall Space Flight Center, Contract NAS8-20082. This task was performed in response to the requirement of Appendix B-1, Schedule Order 129, Para. A, and at the request of Mr. Keith Henson, S&E-AERO-AD.

CONTENTS

Section 1
INTRODUCTION AND SUMMARY

Command Service Module Reaction Control System (CSM/RCS) of the orbital cluster arrangement scheduled for use in the Apollo Applications Program (AAP) contains 16 Reaction Control Motors (RCM) located on the Service Module (SM). When one or more of these motors are fired to effect an attitude change, the exhaust plume will impinge on various surfaces of the cluster. The loadings and moments produced by the plume impingement could cause problems that might affect mission effectiveness; they also require that additional propellant be carried onboard to counteract the thrust cancellation of the plume impinging on the various surfaces.

The current timelines for the Dry Workshop mission shows the Apollo Telescope Mount (ATM) solar panels being deployed prior to the Command Service Module (CSM) docking maneuvers. This requires the ATM solar panels to be able to withstand the resulting CSM-RCS plume impingement loading and thermal environment.

This document presents the results of an analytical investigation to determine the impingement characteristics for six cases of an RCS motor located on the SM being fired for attitude control. These impingement characteristics represent the highest loadings to be expected when the CSM is in the docked position. It is to be noted that an inifinite number of positions from which an attitude control motor might be fired are described as the envelope of possible docking trajectories, some of which might possibly represent higher panel loadings than presented. These cases will be analyzed when the envelope of docking maneuvers is defined. Other roll attitudes for the CSM will also be investigated.

For the cases which were analyzed in the present study, the LM/ATM solar panels will experience maximum impingement loadings of 17.75 lb_f and 14.70 lb_f when motors located on RCS Quads B and C (Fig. 2), respectively, are fired in such a manner that the exhaust plume is directed toward the solar panel.

Section 2
PLUME IMPINGEMENT ANALYSIS

The RCS on the Command Service Module (CSM) uses Marquardt R4D motors with monomethyldrazine and nitrogen tetroxide propellants for attitude control purposes. When these motors are fired to effect an attitude change, the maneuver will result in the exhaust plume impinging on the: (1) CSM; (2) Multiple Docking Adapter (MDA); (3) Apollo Telescope Mount (ATM); (4) forward shoulder of the S-IVB stage; and (5) one or more of the panels of the LM/ATM solar array. Calculations were made to determine the forces and moments resulting from the exhaust plume(s) impinging on these surfaces.

2.1 PROBLEM GEOMETRY

The geometrical orientation of the cluster arrangement is presented in Fig. 1. Each of the four RCS quads (Fig. 2) is located at the same point on the vehicle axis (Fig. 3), with the quads 90 deg apart in the Y-Z plane (Fig. 2). They are offset from the CSM coordinate axes Y, Z (Fig. 2) by a rotation of 7.25 deg about the longitudinal axis of the vehicle (X axis) with the centerline of each engine canted 10 deg to the local surface tangent. Note that the CSM Y-Z axis is rotated 45 deg in a counterclockwise direction (Fig. 2) with respect to the reference Y-Z plane. The reference coordinate system for the respective forces and moments has its origin on the composite vehicle axis of revolution at the J-2 gimbal station (Fig. 3).

In the plume impingement analysis, the various components of the configuration were represented by three basic shapes – a flat plate, cylinder or a conical frustum. The solar panels were considered as rectangular flat plates with the centerline of each plane offset from the reference X axis by a 45-deg rotation about the Z axis. Cylinders were used to represent the Service

Module (SM) and MDA, and the Command Module (CM) and S-IVB stage forward shoulder are represented by conical frustums. The ATM was represented by a cylindrical body.

For this study, six cases of an RCS motor (Ref. 7) being fired were considered. These were for an engine being fired in the vehicle longitudinal direction and in the direction of the solar panels from the SM engine quads (Fig. 2).

2.2 DEFINITION OF THE PLUME IMPINGEMENT CHARACTERISTICS

The impingement characteristics were calculated by Lockheed's Plume Impingement Computer Program (Ref. 1). Basically, the procedure for obtaining the impingement characteristics is as follows. Each body and the particular motor are located with respect to the reference coordinate system. Bodies represented by flat plates are divided into a series of rectangles, and conical shaped bodies are divided into a series of rings with each ring further divided into a given number of radial increments. Local flow conditions on a given body are obtained by locating the centroid of each elemental area in the free plume (Ref. 2) from a search of the plume flow field which is stored on magnetic tape. The flow properties thus obtained are assumed to act uniformly over the elemental areas.

The body local flow regimes were determined by the value of the local Knudsen number. In this analysis, continuum flow was assumed to exist for Knudsen numbers less than 0.01; transitional flow exists for Knudsen numbers between 0.01 and 10.0; and Knudsen numbers greater than 10.0 defines the "free molecular flow" regime. Characteristic lengths used in the Knudsen number calculations (see Ref. 1) were a representative dimension of the body in question so that the elemental area local flow regime is determined by comparing the mean free molecular path of the local plume to the body dimension. The analysis assumed the panels to be flat plates of an infinitesimally small thickness. The centerline of each panel is offset from the reference X axis by a 45-deg rotation about the reference Z axis with the panel 270 in. from the reference X axis. Each panel was represented in the numerical integration scheme by a series of rectangles each 10.5 in. by 10.45 in. (109.72 sq in.) where uniform flow was assumed to exist over each elemental area. The CM and MDA were represented by conical frustums. Each cylinder or frustum was divided into 10 rings with each ring subdivided into 6-deg radial increments. The ATM was represented by a cylinder as shown in Fig. 3, with the body subdivisions for the respective surfaces being 10 rings at 10-deg radial increments for the cylinders. Uniform flow was assumed to exist over each elemental area of the respective surfaces, with orbital conditions considered to exist on the surfaces not exposed to the engine exhaust plume. Characteristic dimensions used in the Knudsen number calculations to determine the surface local flow regime were the panel dimensions and the diameters and lengths of the conical shaped bodies. Also, a representative plume molecular diameter of 0.1×10^{-6} in. was used in the Knudsen number calculations. It should be noted that the force integration results reflect the assumptions used to generate the engine exhaust plume (Ref. 2).

2.3 PLUME IMPINGEMENT FLOW REGIMES

In the continuum regime, the local impact pressures were calculated from a modified Newtonian impact theory (Ref. 3) as given by

$$P_{imp} = P_{\infty}\left(1 + \frac{\gamma}{2} K M_{\infty}^2 \sin^2\alpha\right) \qquad (1)$$

with K given by

$$K = C_{P_s}\left(.814 + \frac{6.88}{\alpha^{4/5}}\right) \qquad (2)$$

where

α = local impingement angle of velocity vector with respect to the local body tangent

P_{imp} = impact pressure

M_N = free stream Mach number

P_∞ = local freestream static pressure

C_{P_s} = stagnation pressure coefficient behind a normal shock.

Fundamental Newtonian theory assumes that the force felt by the body is due to the time rate of change of the normal momentum and is independent of the angle of incidence of the body surface so that there is no transfer of the tangential momentum. The parameter K is included to account for the higher pressures noted experimentally (Ref. 3) for small-incidence angles on flat plates. For this analysis, K ranged from 1.8 to 6.0 and was set to 6.0 for local incidence angles less than 3 deg. The forces and moments were then obtained by numerically integrating the local impact pressure distribution over the body.

The free molecular flow regime is characterized by the fact that the local properties on the body depend only upon collisions of the gas molecules with the body surface. The program of Ref. 1 assumes environmental equilibrium so that a Maxwellian-type flow exists and the local flow properties are calculated from kinetic theory and Maxwell's law of distribution of molecular velocities. The local force on the elemental area is obtained by computing the forces produced by the incident and reflected molecules and adding them. The force is given by

$$\frac{dF}{dA} = \frac{\xi}{2\beta}\left\{\frac{1}{\sqrt{\pi}}(ke + \ell\gamma + t\eta)\left[\gamma S^2\sqrt{\pi}(1 + \mathrm{erf}(\gamma S) + Se^{-\gamma^2 S^2}\right]\right.$$

$$\left. + \frac{\ell}{2}(1 + \mathrm{erf}(\gamma S) + \frac{\ell}{2}\sqrt{\frac{T_R}{T_i}}\left[\gamma S\sqrt{\pi}(1 + \mathrm{erf}(\gamma S) + e^{-\gamma^2 S^2}\right]\right\} \quad (3)$$

where

ξ = density of the molecules
β = $1/2\ RT_R$
R = gas constant
T_i = incident molecular temperature
T_R = reflected molecular temperature and is equal to the body temperature for complete energy accommodation
S = molecular speed ratio
S = mass velocity/most probable molecular velocity
S = $V/\sqrt{2RT_R}$
k, ℓ, t = direction cosines between the local X, Y, Z axes and the force direction
e, γ, η = direction cosines between the local X, Y, Z axes and the mass velocity
$\mathrm{erf}(\gamma S)$ = the error function of S.

The total force in the free molecular regime is obtained by numerically integrating Eq.(3) over the body surface. A detailed development of Eq. (3) is given in Ref. 4.

In the transitional flow regime the local force is calculated from the following empirical expression (Ref. 8)

$$P_{tran} = P_{cont} + (P_{f.m.} - P_{cont})\sin^2\left[\pi(1/3 + 1/6\log_{10}K_n)\right] \quad (4)$$

where

$P_{f.m.}$ = free molecular impact pressure, dF/dA, Eq.(3)

P_{tran} = transitional impact pressure

P_{cont} = continuum impact pressure, Eq.(1)

K_n = local Knudsen number for transitional flow, $0.01 < K_n < 10.0$.

Equation (4) is a function of Mach number and Knudsen number and yields a smooth transition from the continuum to the free molecular flow regime.

Section 3
RESULTS OF THE PLUME IMPINGEMENT ANALYSIS

Impingement forces and moments for the four cases of a control motor firing are presented in Figs. 4 through 9. These cases do not represent the firing sequence, but represent the highest loadings to the composite vehicle for a respective single engine firing while the CSM is in the docked position. (See Section 1.) The highest structural loadings are obtained when an engine is fired in such a manner that the exhaust plume is directed toward an LM/ATM solar panel (Figs. 4 and 6). The maximum predicted loading (Fig. 6) is for a motor located on RCS Quad C (Fig. 2) firing in the direction of the panels 1 and 2 (Fig. 3). The panel integrated force is 17.75 lb_f acting in the direction of the negative Z axis, while the vehicle-integrated impingement force for this case represents a thrust loss of 27.1% in the reference Z direction. For the case presented in Fig. 4, the panel-integrated force is 14.90 lb_f acting in the negative Z direction with the vehicle-integrated impingement force representing a 16% thrust loss in the reference Z direction. The large solar panel loading results from the respective motors firing almost directly at the LM/ATM solar panels, where the impingement angles of the local flow velocity vectors ranged from 45 deg to 74 deg. Panel impingement loadings are somewhat less than those predicted in Ref. 9. This is because the panels are closer to the respective motors by approximately 70 in. The local impact pressure distribution is higher than that calculated in Ref. 9, however, because the panels are closer to the motors in the Dry Workshop resulting in a smaller area of the panel being impinged on by the exhaust plume. The net effect of the larger impact pressure distributions and the smaller impinged area is a reduction in the panel integrated force as compared to the forces of Ref. 9.

Figures 8 and 9 present plume impingement data that result when a reaction control motor located on Quads A and D (Fig. 2), respectively, are fired for attitude control. These motors are located on each quad (Fig. 2) such that the exhaust plumes are directed toward the LM/ATM solar panel. The presence of the SM was not considered in the integration of the panel impingement forces. The panel plume impingement blockage of the SM is estimated to reduce the integrated panel force (Fig. 8) by ≈30% and the Y component of the center-of-pressure vector will shift ≈5% in the negative Y direction. The panel integrated force (Fig. 9) will be reduced by ≈40% due to SM plume blockage with the center-of-pressure component CP_Y shifted ≈5% in the positive Y direction. These approximate corrections are reflected in the data of Figs. 8 and 9.

The integrated forces and moments for the configuration components are presented in tabulated form. The resultant force vector for a given engine(s) firing is given by

$$F_{resultant} = \sum_{\ell=1}^{m} F_{x_\ell} \hat{i} + \sum_{\ell=1}^{m} F_{Y_\ell} \hat{j} + \sum_{\ell=1}^{m} F_{Z_\ell} \hat{k} \qquad (5)$$

where

$\hat{i}, \hat{j}, \hat{k}$ are unit vectors in the reference X, Y, Z directions, respectively

$\sum_{\ell=1}^{m}$ indicates summation of all contributing vector components, i.e., SM, MDA, panel, etc., for all engine or engine combinations considered.

Similarily, the resultant moments produced by the resultant impingement force is

$$M_{resultant} = \sum_{\ell=1}^{m} M_{X_\ell} \hat{i} + \sum_{\ell=1}^{m} M_{Y_\ell} \hat{j} + \sum_{\ell=1}^{m} M_{Z_\ell} \hat{k} \qquad (6)$$

where the individual terms are defined in a fashion similar to Eq.(5). It is to be noted that when combining the forces due to two or more engines firing there is the possibility that plume interactions might exist. To account for this, however, would require that any three-dimensional effects and shock interactions be included which is beyond the scope of the current planned effort.

The impingement calculations assume the flow field to be inviscid. Therefore, any boundary layer effects which produce plume impingement outside the calculated plume boundary are disregarded as is any viscous (skin) forces between the plume and the respective bodies.

The assumptions made to generate the plume flow field and the numerical integration scheme introduce some inaccuracies into the data. Reference 4 indicates the overall percentage error for the undisturbed flow field to be approximately $\pm 20\%$ and the numerical integration scheme used to obtain the impingement data should introduce a percentage error of less than $\pm 10\%$. The Newtonian pressure coefficients were obtained from a curve fit of high-speed flow impinging on a flat plate and should be accurate to $\pm 5\%$. Three-dimensional flow effects introduce additional accuracy bands whose magnitudes depend upon the location of the body in the plume. Three-dimensional flow effects on the solar panel impingement forces are estimated to introduce an accuracy band of approximately $\pm 25\%$. The rms summation of these accuracy bands results in an overall band of approximately $\pm 35\%$. A more rigorous analysis of the OWS impingement characteristics will require: (1) that body shadowing be included in the impingement calculations; (2) that the local flow properties reflect any three-dimensional effects due to the engine plume attaching to an expanding around the S-IVB stage; and (3) that local skin friction forces be included.

REFERENCES

1. Butler, H. W., "Description and User's Manual for a Program to Analyze Loads and Heating on Bodies Subject to Rocket Exhaust Plume Impingement," LMSC/HREC A791231, Lockheed Missiles & Space Company, Huntsville, Ala., February 1968.

2. Jackson, J. E., "Preliminary Data for Plume Definition of the R4D Engine for the Command Service Module Reaction Control Systems," LMSC/HREC A791774, Lockheed Missiles & Space Company, Huntsville, Ala., 13 September 1968

3. Buck, M. L. and E. J. McLaughlin, "A Technique for Predicting Pressure Distributions and Aerodynamic Force Coefficients for Hypersonic Wing Reentry Vehicles (U)," ASP-TDR-63-552, August 1963 (Confidential).

4. Sentman, Lee H., "Free Molecular Flow Theory and Its Application to the Determination of Aerodynamic Forces," LMSC-448514, Lockheed Missiles & Space Company, Sunnyvale, Calif., October 1961.

5. Ratliff, A. W., "Estimation of Accuracy of Flow Field Variable," Lockheed Missiles & Space Company, Huntsville, Ala. (to be published.)

6. Peters, W., Private Communications, NASA-Manned Spacecraft Center, Houston, Texas, June 1968.

7. Baker, L. R., "Summary of Engine Characteristics Considered in Plume Definition Study," TN 54/20-36, LMSC/HREC A791937, Lockheed Missiles & Space Company, Huntsville, Ala., October 1968.

8. Ratliff, A. W., et. al., "Analysis of Heating Rates and Forces on Bodies Subject to Rocket Exhaust Plume Impingement," LMSC/HREC A791230, HREC-1150-1, Lockheed Missiles & Space Company, Huntsville, Ala., March 1968.

9. Penny, M. M., "Forces Due to a Command Service Module Reaction Control Motor Plume Impinging on the AAP Cluster Arrangement," LMSC/HREC D148850, Lockheed Missiles & Space Company, Huntsville, Ala., April 1969.

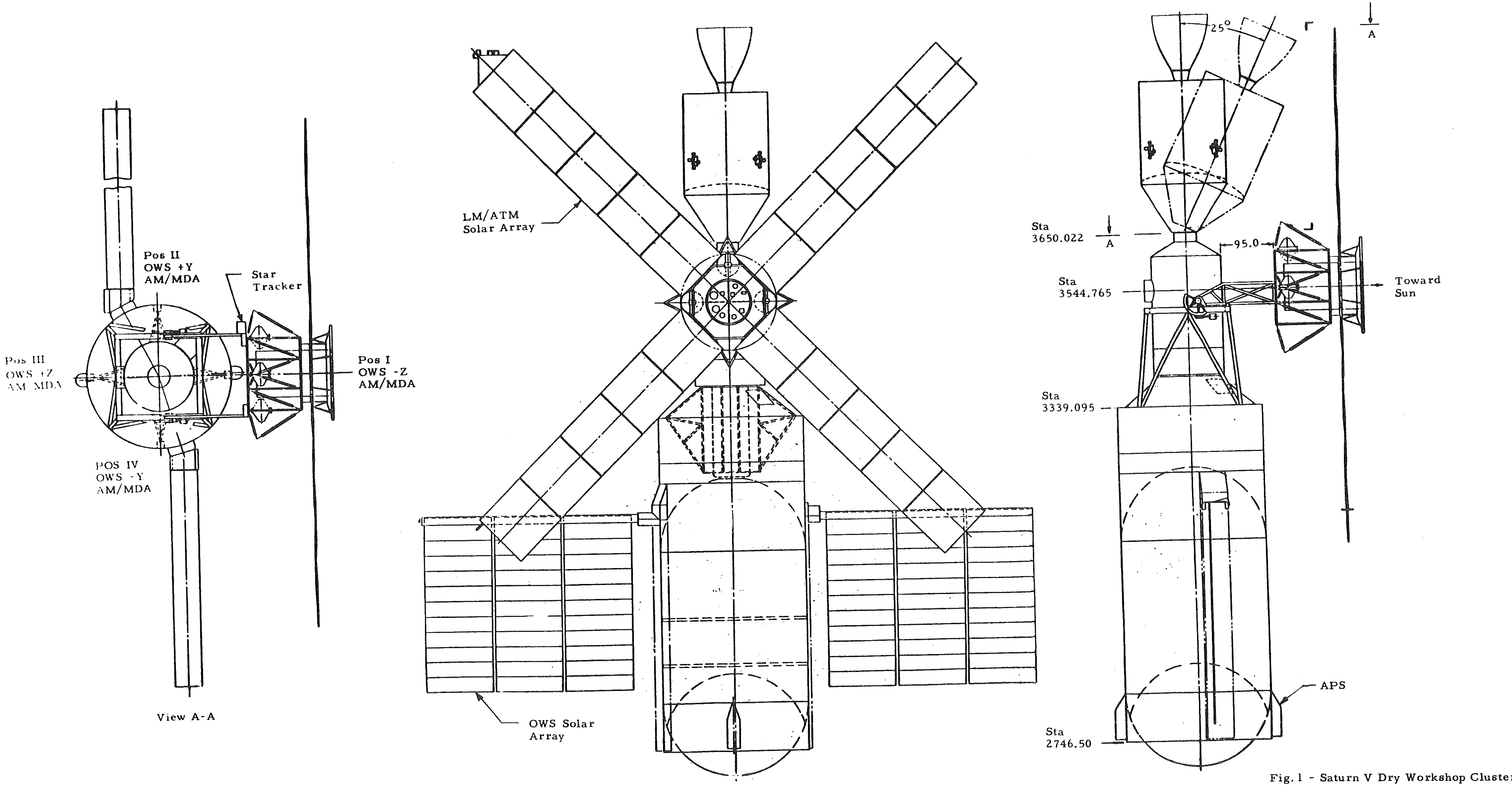

Fig. 1 - Saturn V Dry Workshop Cluster Arrangement

*RCS denotes reaction control system. There are four engines per RCS quad. Quad designation is obtained from Ref. 6.

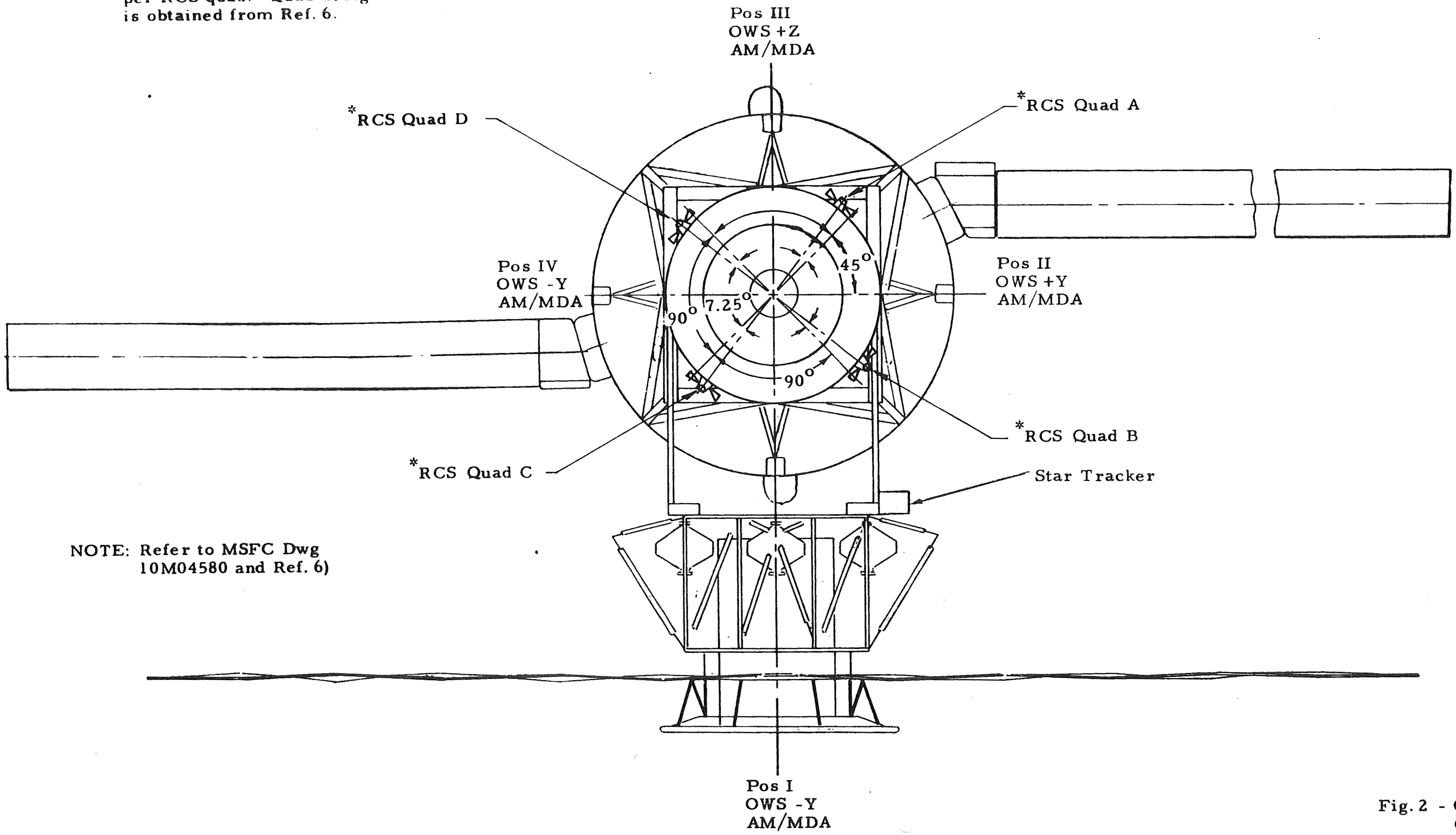

NOTE: Refer to MSFC Dwg 10M04580 and Ref. 6)

Fig. 2 - Orientation of CSM Reaction Control System.

NOTES:

1. Dimensions are in inches
2. Roman numerals I, II, III, IV indicate launch vehicle axes -Z, +Y, +Z and -Y, respectively
3. Drawing not to scale
4. Reference MSFC Dwg. 10M04580

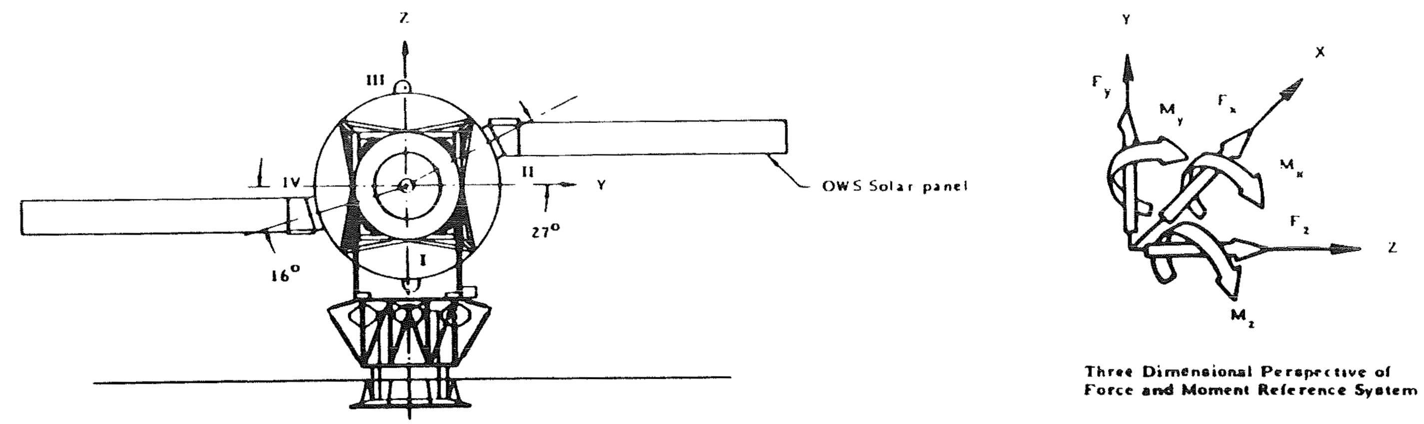

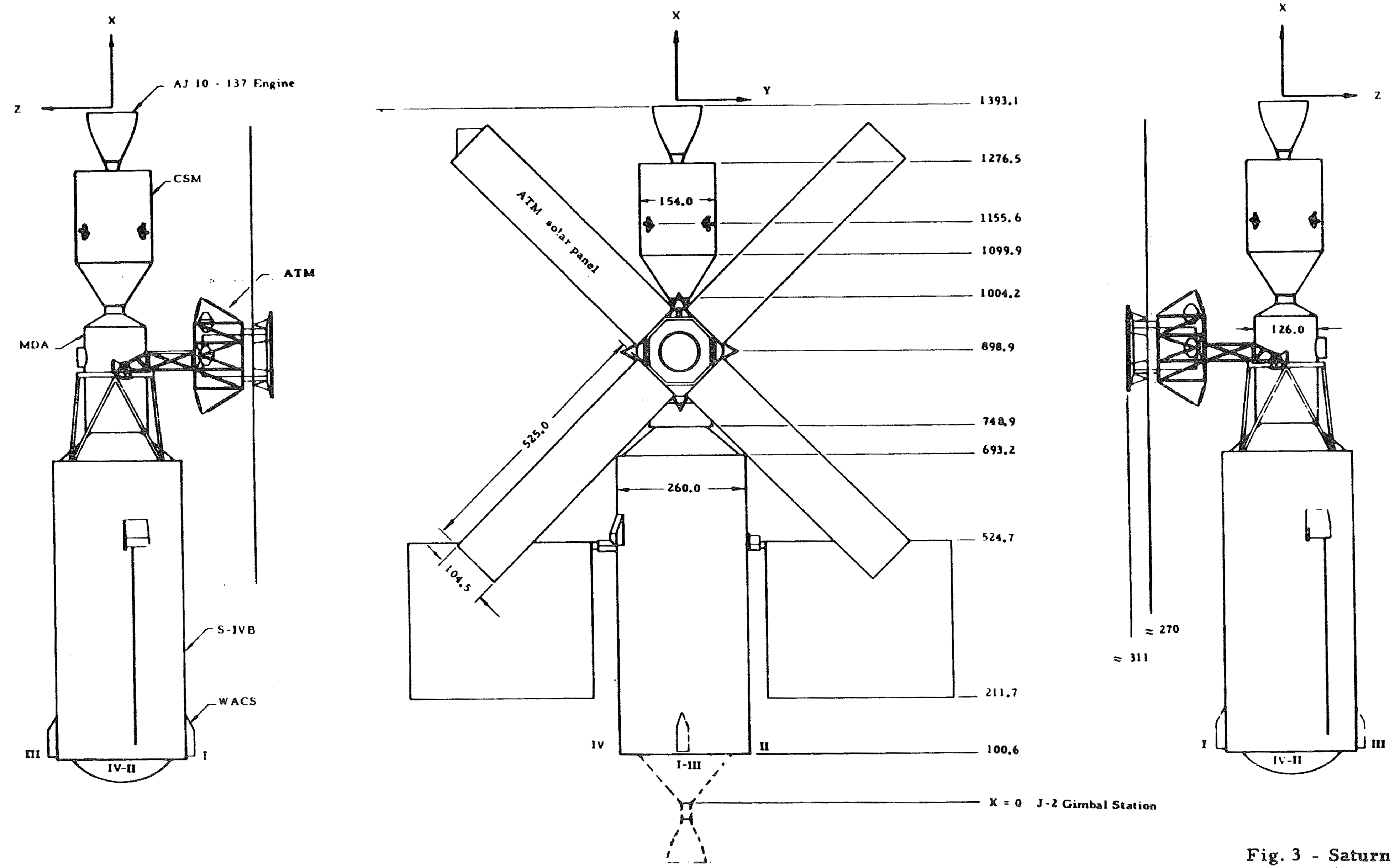

Fig. 3 - Saturn V Dry Workshop Cluster Arrangement and Reference Coordinate System for Plume Impingement Data

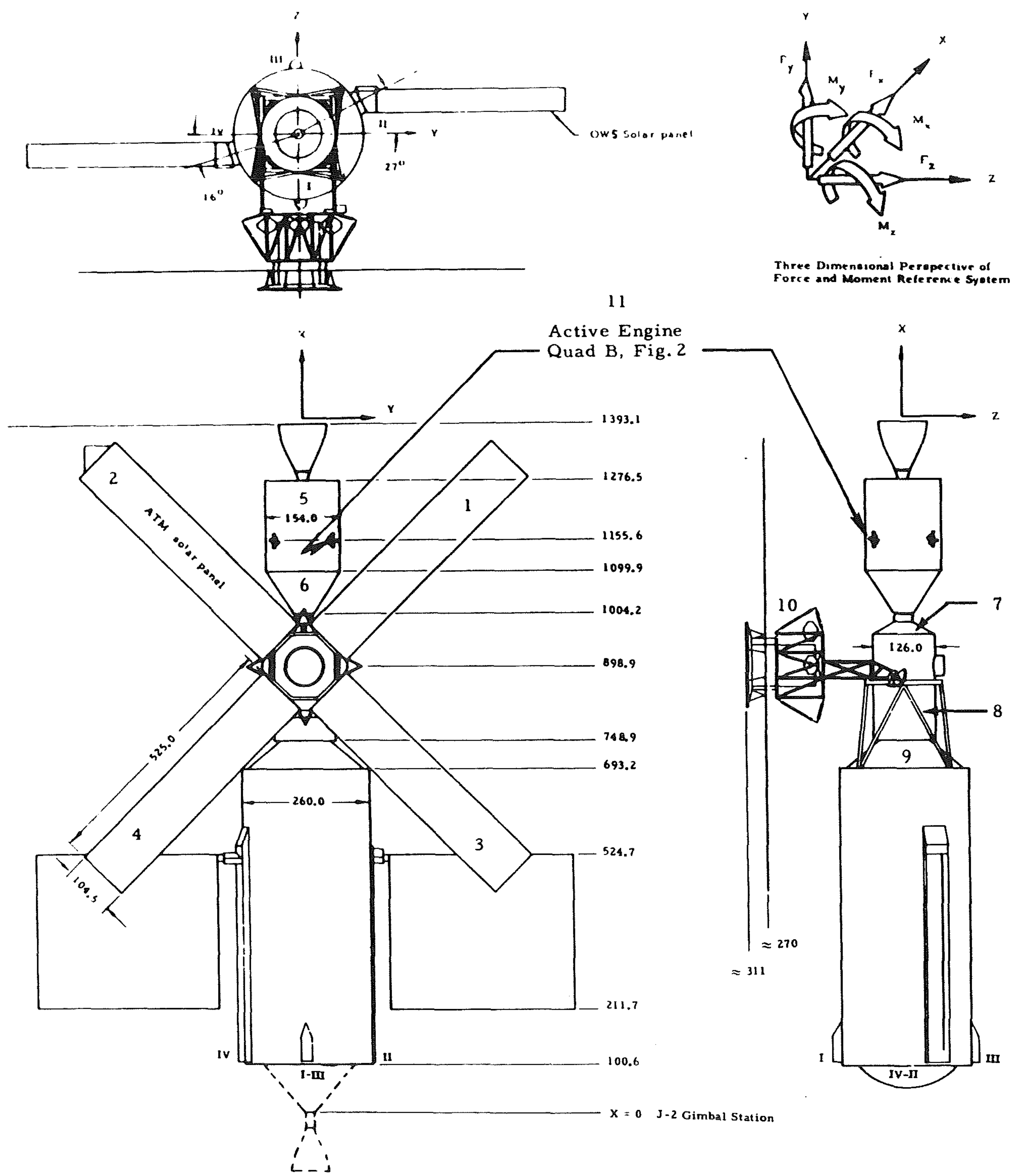

NOTES:

1. $\overrightarrow{CP}$ is the location of the integrated resultant plume impingement pressure force
2. Moments and $\overrightarrow{CP}$ referenced to the J-2 gimbal station
3. Roman numerals I, II, III, IV indicate launch vehicle axes -Z, +Y, +Z and -Y, respectively
4. Refer to MSFC Drawing 10M04580 and Ref. 6
5. Drawing not to scale
6. R4D engine theoretical thrust ≈ 105 lb_f (Ref. 2) (vacuum thrust)

* (1) Angular orientation of resultant force is 37.17 deg off Position I toward Position II

* (2) Angular orientation of resultant force is 9.1 deg off Position I toward Position II

Body No.	Item	F_x	F_y	F_z	M_x	M_y	M_z	CP_x	CP_y	CP_z
		lb_f	lb_f	lb_f	ft-lb_f	ft-lb_f	ft-lb_f	ft	ft	ft
1	Solar Panel	0.0	0.0	-2.84	-22.07	243.22	0.0	85.64	7.77	-22.5
2	Solar Panel	0.0	0.0	-12.06	162.57	1082.02	0.0	89.72	-13.48	-22.5
3	Solar Panel	Body is outside theoretical plume boundary or shaded by another body(s)								
4	Solar Panel	Body is outside theoretical plume boundary of shaded by another body(s)								
5	SM	0.0	-1.46	1.91	0.0	-182.20	-139.34	95.31	*(1)	*(1)
6	CM	0.01	-0.01	0.06	0.0	- 6.03	- 0.21	87.50	*(2)	*(2)
7	MDA Forward Shoulder	Body is outside theoretical plume boundary or shaded by another body(s)								
8	MDA	Body is outside theoretical plume boundary or shaded by another body(s)								
9	S-IVB Forward Shoulder	Body is outside theoretical plume boundary or shaded by another body(s)								
10	ATM	-1.0	-.26	0.0	-4.29	16.50	-20.39	74.91	-.91	-16.50
11	R4D Engine	0.0	48.83	92.91	720.05	-8949.39	4639.58	96.32	5.24	-4.76

Fig. 4 - Resulting Forces and Moments Due to a CSM Reaction Control Motor (R4-D) Firing in Quadrants II-III in the Direction of the Solar Panel Array

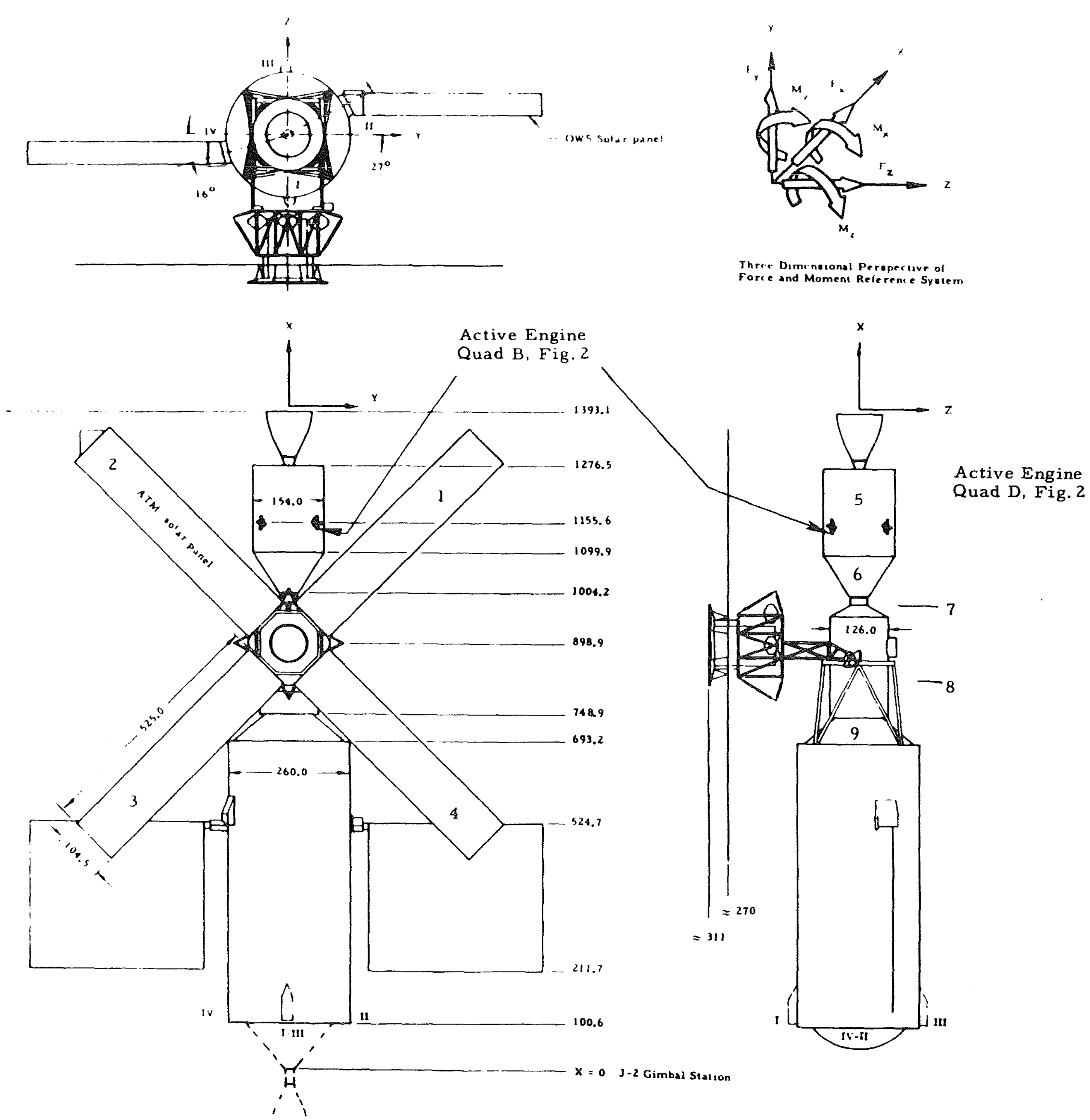

NOTES:

1. $\overrightarrow{CP}$ is the location of the integrated resultant plume impingement pressure force with respect to the reference coordinate system
2. Moments and $\overrightarrow{CP}$ are referenced to the J-2 gimbal station
3. Roman numerals I, II, III, IV indicate launch vehicle axes -Z, +Y, +Z and -Y, respectively
4. Refer to MSFC Drawing 10M04580 or Ref. 6
5. Drawing not to scale
6. R4D engine theoretical thrust = 105 lb_f, Ref. 2 (vacuum thrust)

* (1) Angular orientation of resultant force is 52.25 deg off Position I toward Position II

* (2) Angular orientation of resultant force is 52.26 deg off Position I toward Position II

* (3) Angular orientation of resultant force is 45.07 deg off Position I toward Position II

* (4) Angular orientation of resultant force is 52.26 deg off Position I toward Position II

* (5) Angular orientation of resultant force is 48.05 deg off Position I toward Position II

Body No.	Item	F_x	F_y	F_z	M_x	M_y	M_z	CP_x	CP_y	CP_z
		lbf	lb_f	lb_f	ft-lb_f	ft-lb_f	ft-lb_f	ft	ft	ft
1	Solar Panel	0.0	0.0	-2.29	-23.01	194.86	0.0	85.09	10.05	-22.05
2	Solar Panel	Body is outside of theoretical plume boundary or shaded by another body(s)								
3	Solar Panel	Body is outside of theoretical plume boundary or shaded by another body(s)								
4	Solar Panel	Body is outside of theoretical plume boundary or shaded by another body(s)								
5	SM	0.0	-7.46	5.83	0.0	-545.19	-696.61	93.47	*(1)	*(1)
6	CM	2.83	-0.95	0.75	0.0	66.25	83.91	88.33	*(2)	*(2)
7	MDA Forward Shoulder	-6.57	-2.38	2.38	0,0	-177.03	-176.45	74.17	*(3)	*(3)
8	MDA	0.0	-0.35	0.28	0.0	-20.81	-26.28	74.12	*(4)	*(4)
9	S-IVB Forward Shoulder	-3.88	-2.03	2.26	0.0	-118.10	-106.14	52.10	*(5)	*(5)
10	ATM	-1.5	-0.39	0.0	-6.50	25.00	-30.58	74.91	-.911	-16.67
11	R4D Engine	103.32	-14.39	11.13	-0.79	-1748.16	-1921.66	94.41	5.45	-4.17

Fig. 5 - Resulting Forces and Moments Due to a CSM Reaction Control Motor (R4-D) Firing in Quadrants I-II (Quad B, Fig. 2) in the Direction of CSM Longitudinal Axis

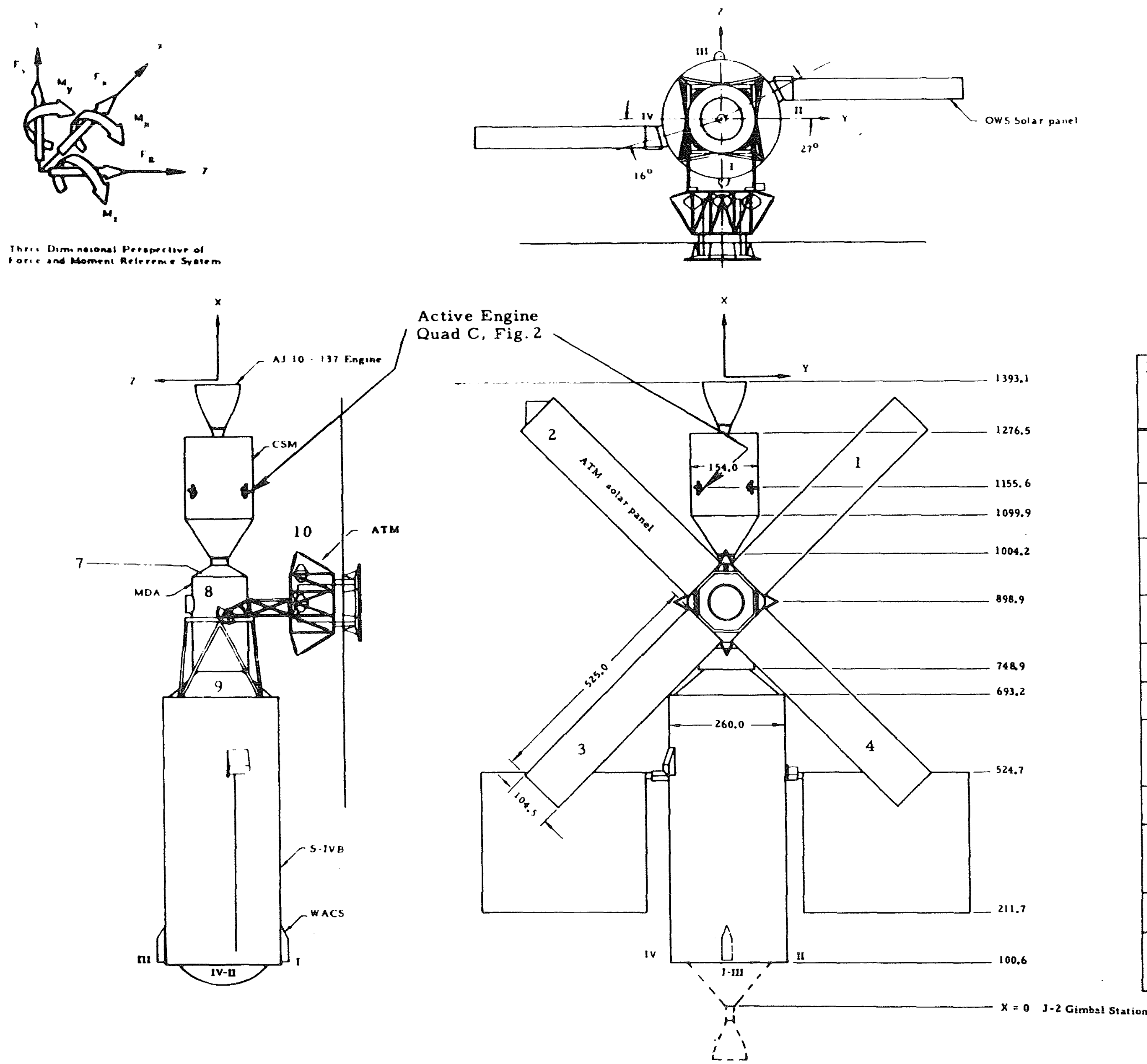

NOTES:

1. $\vec{CP}$ is the location of the integrated resultant plume impingement pressure force with respect to the reference coordinate system
2. Forces, moments and $\vec{CP}$ are referenced to the J-2 gimbal station
3. Roman numerals I, II, III, IV indicate launch vehicle axes -Z, +Y, +Z and -Y, respectively
4. Refer to MSFC Drawing 10M04580 or Ref. 6
5. Drawing not to scale
6. R4D engine theoretical thrust = 105 lb_f (Ref. 2) (vacuum thrust)

* (1) Angular orientation of resultant is 22.31 deg off Position I toward Position IV

* (2) Angular orientation of resultant force is 9.1 deg off Position I toward Position IV

Body No.	Item	F_x	F_y	F_z	M_x	M_y	M_z	CP_x	CP_y	CP_z
		lb_f	lb_f	lb_f	ft-lb_f	ft-lb_f	ft-lb_f	ft	ft	ft
1	Solar Panel	0.0	0.0	-17.59	-267.90	1604.56	0.0	91.22	15.23	-22.50
2	Solar Panel	0.0	0.0	-.16	0.58	13.36	0.0	83.53	-3.63	-22.50
3	Solar Panel	Body is outside of theoretical plume boundary or shaded by another body(s)								
4	Solar Panel	Body is outside of theoretical plume boundary or shaded by another body(s)								
5	SM	0.0	0.89	2.16	0.0	-206.77	84.33	95.33	*(1)	*(1)
6	CM	0.10	0.01	0.06	0.0	-6.05	-0.90	87.50	*(2)	*(2)
7	MDA Forward Shoulder	Body is outside theoretical plume boundary or shaded by another body(s)								
8	MDA	Body is outside theoretical plume boundary or shaded by another body(s)								
9	S-IVB Forward Shoulder	Body is outside theoretical plume boundary or shaded by another body(s)								
10	ATM	-2.9	0.5	0.0	+8.59	49.79	38.19	74.91	-.61	-17.17
11	R4D Engine	0.0	-70.56	77.70	-720.14	-7484.07	-6796.33	96.32	-3.88	-5.92

Fig. 6 - Resulting Forces and Moments Due to a CSM Reaction Control Motor (R4-D) Firing in Quadrants I-IV (Quad C, Fig. 2) in the Direction of the ATM Solar Panel Array

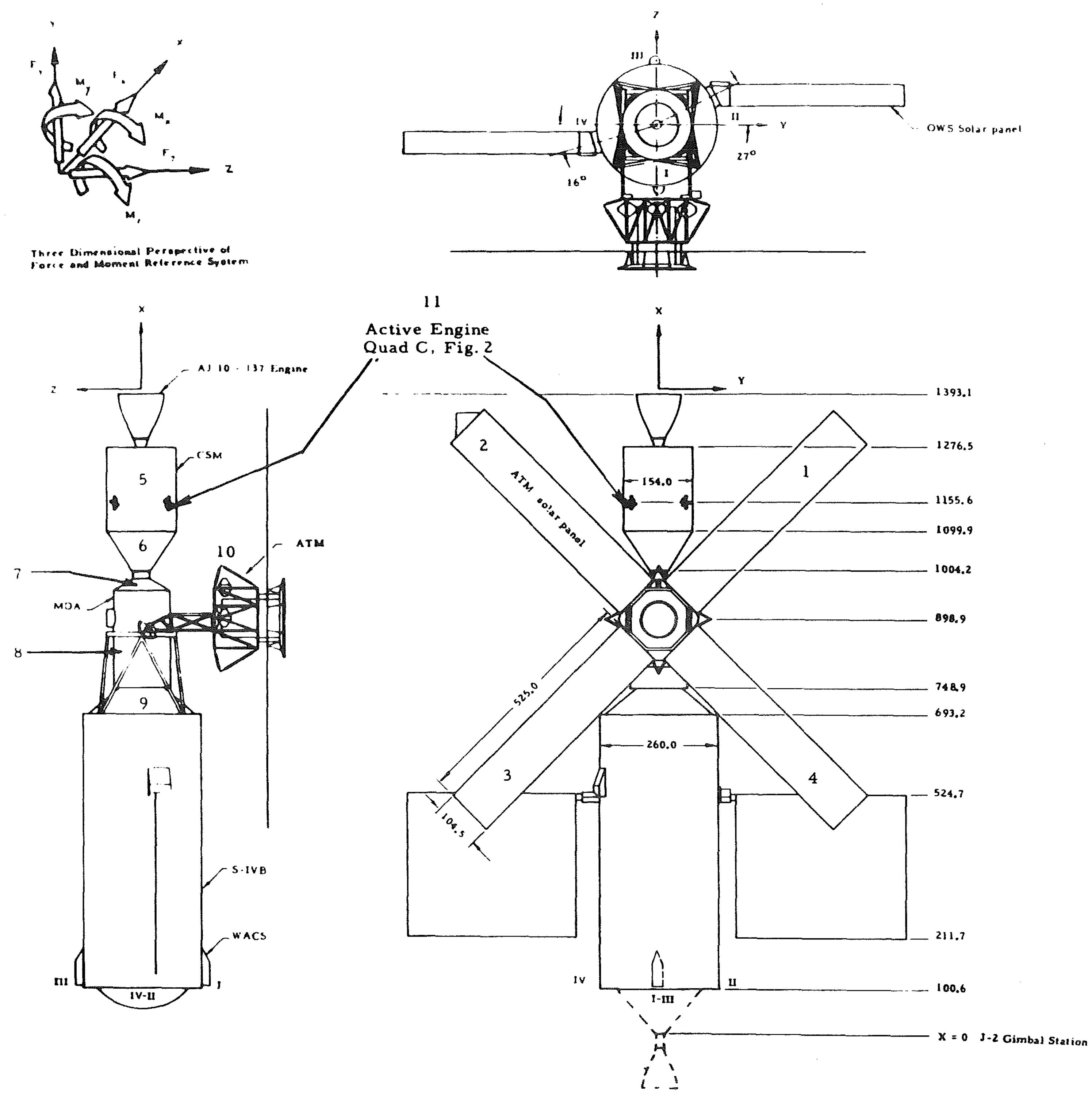

NOTES:

1. $\overrightarrow{CP}$ is the location of the integrated resultant plume impingement pressure force with respect to the reference coordinate system
2. Moments and $\overrightarrow{CP}$ are referenced to the J-2 gimbal station
3. Roman numerals I, II, III, IV indicate launch vehicle axes -Z, +Y, +Z and -Y, respectively
4. Refer to MSFC Drawing 10M04580 or Ref. 6
5. Drawing not to scale
6. R4D engine theoretical thrust = 105 lb_f (Ref. 2) (vacuum thrust)

* (1) Angular orientation of resultant force is 37.64 deg off Position I toward Position IV

* (2) Angular orientation of resultant force is 37.04 deg off Position I toward Position IV

* (3) Angular orientation of resultant force is 37.95 deg off Position I toward Position IV

* (4) Angular orientation of resultant force is 41.84 deg off Position I toward Position IV

* (5) Angular orientation of resultant force is 43.12 deg off Position I toward Position IV

Body No.	Item	F_x	F_y	F_z	M_x	M_y	M_z	CP_x	CP_y	CP_z
		lb_f	lb_f	lb_f	ft-lb_f	ft-lb_f	ft-lb_f	ft	ft	ft
1	Solar Panel	Boundary is outside of theoretical plume boundary or shaded by another body(s)								
2	Solar Panel	0.0	0.0	-1.63	1.17	143.87	0.0	81.01	-7.18	-22.50
3	Solar Panel	Body is outside of theoretical plume boundary or shaded by another body(s)								
4	Solar Panel	Body is outside theoretical plume boundary or shaded by another body(s)								
5	SM	0.0	6.08	7.89	0.0	-737.30	568.70	93.41	*(1)	*(1)
6	CM	2.98	0.92	1.20	0.0	-264.47	81.65	88.75	*(2)	*(2)
7	MDA Forward Shoulder	-6.55	2.38	2.39	0.0	-176.43	177.20	77.25	*(3)	*(3)
8	MDA	0.0	0.36	0.41	0.0	27.73	24.49	63.33	*(4)	*(4)
9	S-IVB Forward Shoulder	-2.31	1.71	1.55	0.0	84.58	93.50	54.39	*(5)	*(5)
10	ATM	-2.5	0.3-	0.0	-5.15	42.9	-20.47	74.08	-0.70	-17.16
11	R4D Engine	103.40	11.16	14.41	0.07	-1930.22	1495.79	94.41	-4.27	-5.52

Fig. 7 - Resulting Forces and Moments Due to a CSM Reaction Control Motor (R4-D) Firing in Quadrants I-IV (Quad C, Fig. 2) in the Direction of the CSM Longitudinal Axis

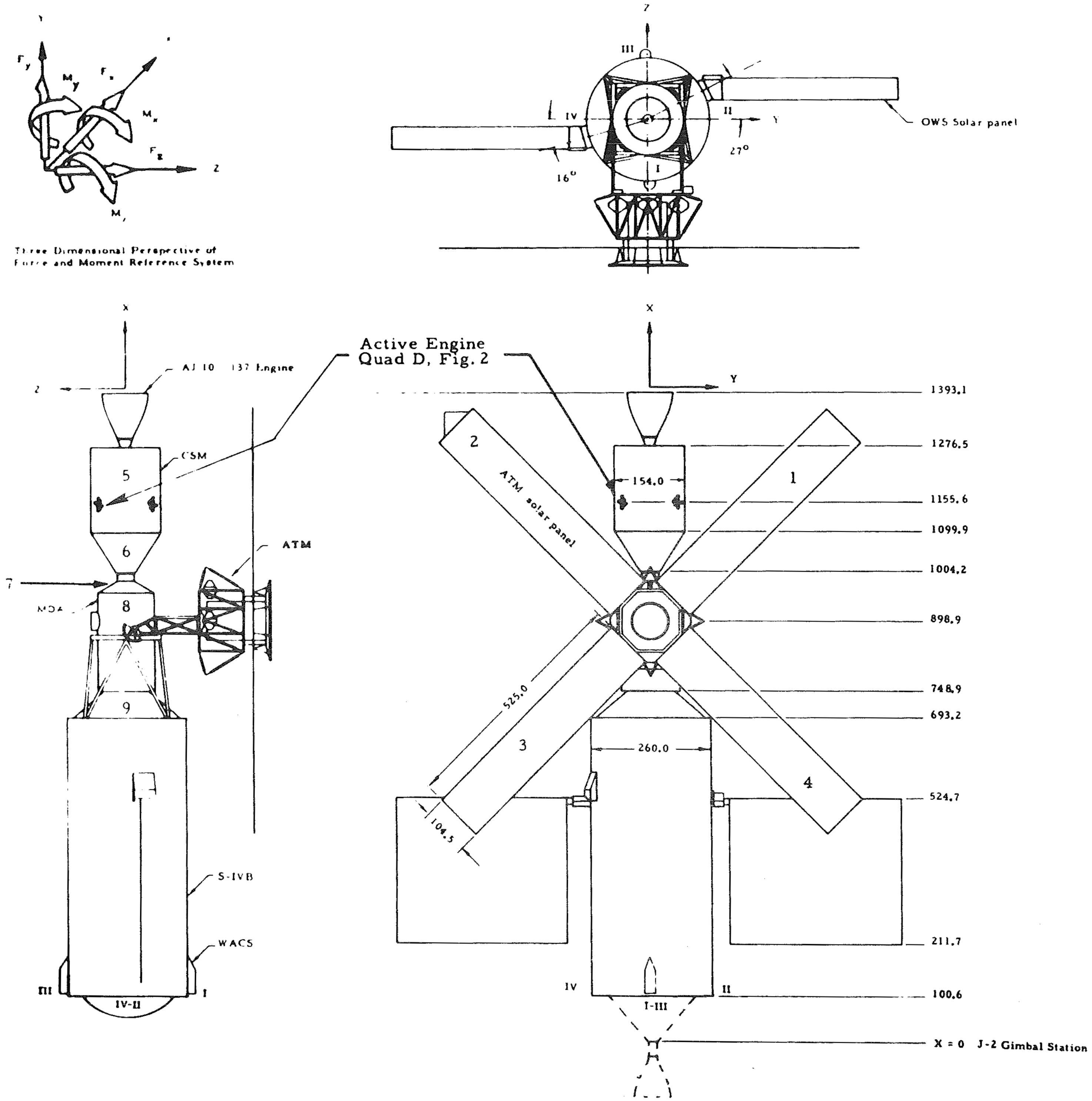

NOTES:

1. $\overrightarrow{CP}$ is the location of the integrated resultant plume impingement pressure force with respect to the reference coordinate system
2. Moments and $\overrightarrow{CP}$ are referenced to the J-2 gimbal station
3. Roman numerals I, II, III, IV indicate launch vehicle axes -Z, +Y, +Z and -Y, respectively
4. Refer to MSFC Drawing 10M04580 or Ref. 6
5. Drawing not to scale
6. R4D engine theoretical thrust = 105 lb_f (Ref. 2) (vacuum thrust)

*(1) Angular orientation of resultant force is 22.3 deg off Position IV toward Position III

*(2) Angular orientation of resultant force is 9.1 deg off Position IV toward Position III

Body No.	Item	F_x	F_y	F_z	M_x	M_y	M_z	CP_x	CP_y	CP_z
		lb_f	lb_f	lb_f	ft-lb_f	ft-lb_f	ft-lb_f	ft	ft	ft
1	Solar Panel	Body is outside theoretical plume boundary or shaded by another body(s)								
2	Solar Panel	0.0	0.0	-13.62	307.54	1313.51	0.0	96.44	-22.58	-22.50
3	Solar Panel	Body is outside theoretical plume boundary or shaded by another body(s)								
4	Solar Panel	Body is outside theoretical plume boundary or shaded by another body(s)								
5	SM	0.0	0.89	-2.16	0.00	206.77	84.85	95.33	*(1)	*(1)
6	CM	0.10	0.01	-0.06	0.0	6.05	0.90	87.50	*(2)	*(2)
7	MDA Forward Shoulder	Body is outside theoretical plume boundary or shaded by another body(s)								
8	MDA	Body is outside theoretical plume boundary or shaded by another body(s)								
9	S-IVB Forward Shoulder	Body is outside theoretical plume boundary or shaded by another body(s)								
10	ATM	Body is outside theoretical plume boundary or shaded by another body(s)								
11	R4D Engine	0.0	70.56	77.70	-719.19	-7484.06	6796.34	96.32	-3.88	5.92

Fig. 8 - Resulting Forces and Moments Due to a CSM Reaction Control Motor (R4-D) Firing in Quadrants I - IV (Quad D, Fig. 2) in the Direction of the ATM Solar Panel Array

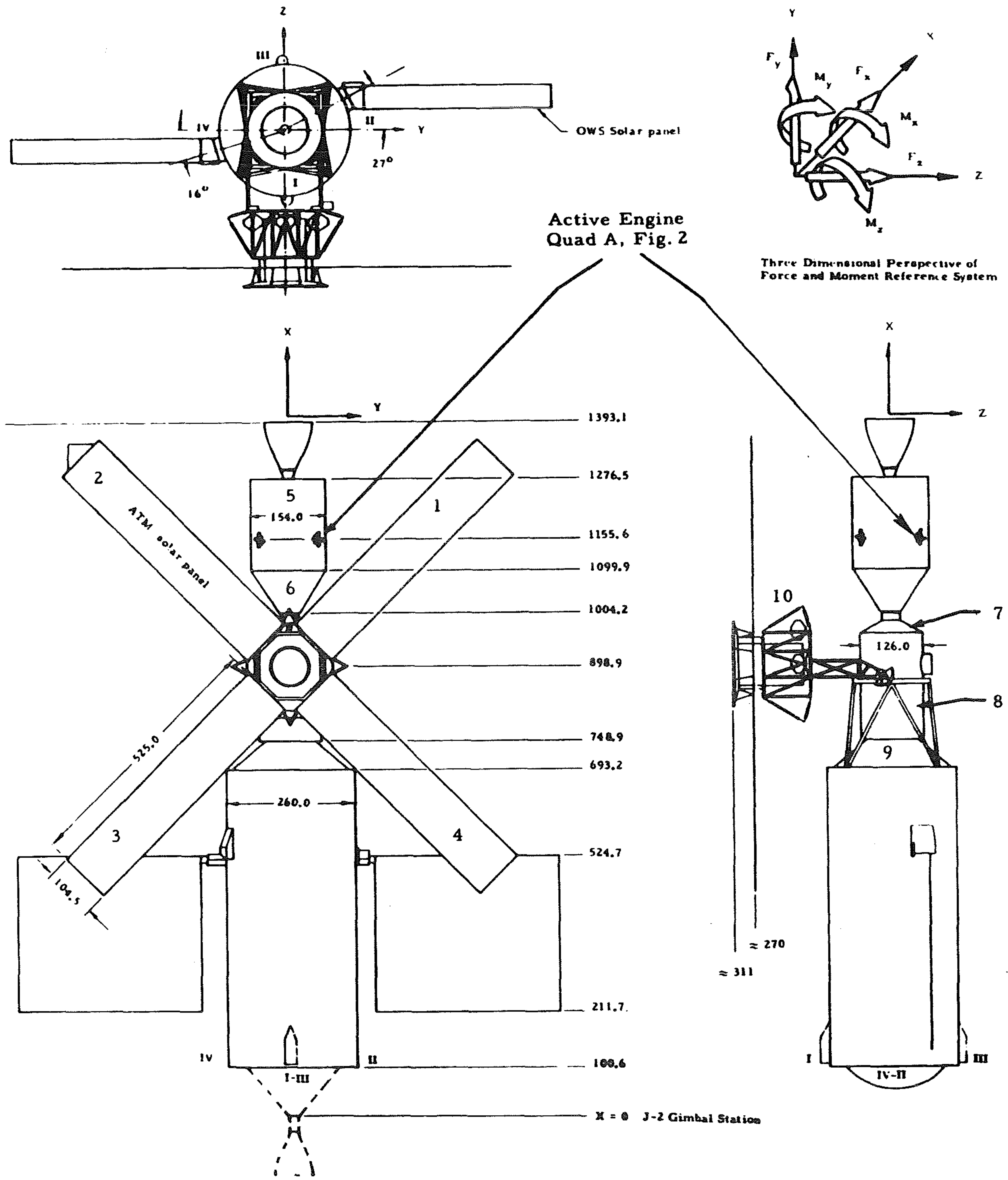

NOTES:

1. $\overrightarrow{CP}$ is the location of the integrated resultant plume impingement pressure force with respect to the reference coordinate system
2. Moments and $\overrightarrow{CP}$ referenced to the J-2 gimbal station
3. Roman numerals I, II, III, IV indicate launch vehicle axes -Z, +Y, +Z and -Y, respectively
4. Refer to MSFC Drawing 10M04580 or Ref. 6
5. Drawing not to scale
6. R4D engine theoretical thrust ≈ 105 lb_f (Ref. 2) (vacuum thrust)

* (1) Angular orientation of resultant force is 22.31 deg off Position II toward Position III

* (2) Angular orientation of resultant force is 9.1 deg off Position II toward Position III

Body No.	Item	F_x lb_f	F_y lb_f	F_z lb_f	M_x ft-lb_f	M_y ft-lb_f	M_z ft-lb_f	CP_x ft	CP_y ft	CP_z ft
1	Solar Panel	0.0	0.0	-2.83	-67.95	244.73	0.0	96.73	21.82	-22.50
2	Solar Panel	Body is outside of the theoretical plume boundary or shaded another body(s)								
3	Solar Panel	Body is outside of the theoretical plume boundary or shaded another body(s)								
4	Solar Panel	Body is outside of the theoretical plume boundary or shaded another body(s)								
5	SM	0.0	-1.46	-1.91	0.0	182.20	-139.34	95.31	*(1)	*(1)
6	CM	0.1	-0.01	-0.06	0.0	6.05	-0.88	87.50	*(2)	*(2)
7	MDA Forward Shoulder	Body is outside of the theoretical plume boundary or shaded another body(s)								
8	MDA	Body is outside of the theoretical plume boundary or shaded another body(s)								
9	S-IVB Forward Shoulder	Body is outside of the theoretical plume boundary or shaded another body(s)								
10	ATM	Body is outside of the theoretical plume boundary or shaded another body(s)								
11	R4D Engine	0.0	-48.83	92.91	719.19	-8949.39	-4703.31	96.32	5.24	4.76

Fig. 9 - Resulting Forces and Moments Due to a CSM Control Motor (R4-D) Firing in Quadrants II-III (Quad A, Fig. 2) Toward the ATM Solar Panel Array